JOURNAL OF MATERIALS SCIENCE 30 (1995) 5927–5930

Effects of 50 keV $^2H^+$-ion implantation and rapid thermal annealing on the microstructure of YBCO thin films

Y. H. LI, C. LEACH, T. J. TATE, M. J. LEE, YUPU LI, J. A. KILNER
Centre for High T_C Superconductivity, Imperial College, London, SW7 2BP, UK
P. G. QUINCEY
National Physical Laboratory, Teddington, Middlesex, TW11 0LW, UK

A YBCO film with thickness of about 200 nm was deposited on $LaAlO_3$ [1 0 0] by direct current (d.c.) sputtering. The film, which was found to be mainly *c*-axis orientated, was irradiated at room temperature with 50 keV $^2H^+$ ions to a dose of 1×10^{16} cm^{-2}. This implantation destroyed the superconductivity and made the film textured, with the "epitaxial" crystalline structure of the film being mainly maintained. Transmission electron microscope studies show that there are a considerable number of amorphous islands, which are Y rich and Cu poor compared with the 1 2 3 phase in the as-received YBCO film. These amorphous islands are found to be unstable under the irradiation, as after implantation some polycrystalline regions, rather than amorphous islands, can be seen by TEM. Rapid thermal annealing in flowing O_2 ambient can induce oxygen reordering and results in partial recovery of critical temperature, T_C. After RTA, the polycrystalline regions have not changed.

1. Introduction

Hydrogen ion implantation into superconducting films introduces damage which, depending on the energy and dose of the implanted ions, can either enhance flux pinning so as to increase critical current (J_c), or otherwise decrease critical temperature (T_c) and destroy superconductivity [1,2]. Rapid thermal annealing (RTA) can recover the excessive damage due to ion implantation and at the same time avoid interdiffusion between film and substrate, since the annealing time is very short. Therefore it is important to understand the effects of the ion implantation and RTA on the microstructure of the film. High resolution and analytical transmission electron microscopy (TEM) is a powerful tool used in the study of crystalline structures, and has been extensively used in microstructure analysis of thin films.

In this paper is reported the effect of 50 keV $^2H^+$ ion implantation and rapid thermal annealing on the microstructure of YBCO thin films, based mainly on results from TEM observations.

2. Experimental procedure

A YBCO film, approximately 200 nm thick was deposited onto $LaAlO_3$ [1 0 0] substrates *in situ* by d.c. sputtering from a stoichiometric target, using the inverted cylindrical magnetron method [3]. The substrate was clamped to a resistive heater, with copper shim to improve thermal contact. During deposition of the films, the temperature of the heater block was about 840 °C. After deposition the chamber was back-filled to 205×10^4 Pa of oxygen, and the sample allowed to cool to about 450 °C over 15 min before the heater was switched off.

Implantation was performed with 50 keV $^2H^+$ ions to a dose of 1×10^{16} cm^{-2} at room temperature, at 7° to the surface normal. After implantation the sample was subdivided into $\sim 2 \times 3$ mm^2 pieces and some of them were annealed in a pure flowing oxygen ambient in an RTA oven, at a nominal temperature of 870 °C. During RTA, it took less than 4 s for the temperature to increase linearly to the set temperature. Therefore the shortest annealing time, (i.e. 20 s) is at least five times longer than the ramp time.

Plan view samples for TEM were made by mechanical thinning, dimpling and ion milling from the back side of the substrates. Cross-section samples were prepared by gluing the samples film to film. After mechanical thinning the samples were dimpled to about 10 μm thick in the central area and ion milled to perforation.

3. Results and discussion

A plan view image of the as-received film without $^2H^+$ ion implantation and annealing is shown in Fig. 1. The electron beam diffraction pattern shows that most of it is a *c*-axis orientated epitaxial structure of the 1 2 3 phase. However, even though the T_c of the film is as high as 89 K, there are a lot of bright islands distributed through out the whole film, some of which are indicated by A in Fig. 1. Microbeam diffraction patterns of the islands reveal that these regions are

0022–2461

mainly amorphous, as shown in an insert. Chemical analysis of the islands by energy dispersive X-rays shows that they are Y rich and Cu poor compared with the 1 2 3 phase [4].

Fig. 2 shows a high resolution cross-section image of the non-implanted sample, which shows an amorphous area (indicated by A) near the substrate with a second phase precipitate (indicated by an arrow). This kind of second phase has been identified by Catana *et al.* as cubic Y_2O_3 (a =1.06 nm) [5]. The orientation of the precipitate is (1 0 0)Y_2O_3//[1 0 0] substrate and [0 1 1] Y_2O_3//[0 0 1] substrate. This is because the (1 0 0) substrate plane has the smallest lattice mismatch to (1 0 0)Y_2O_3 (1.1%) along [0 1 1]Y_2O_3//[0 0 1] substrate ($LaAlO_3$ is pseudo-cubic with a =0.379 nm). These small precipitates were observed throughout the Y rich and Cu poor amorphous area. Some c-axis orientated epitaxial 1 2 3 phase can be seen as well in the figure (indicated Y).

Fig. 3 shows a group of plan view TEM micrographs and selected area diffraction patterns of the film after implantation. Fig. 3a shows a low magnification image. Some polycrystalline rather than

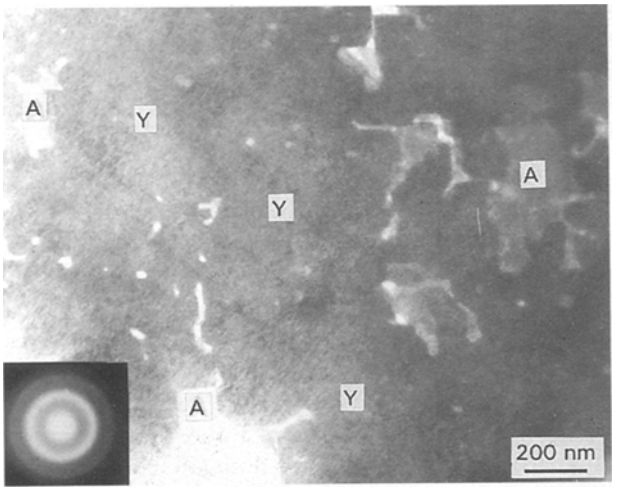

Figure 1 Plan view TEM micrograph of the as-deposited YBCO film, and, insert, corresponding selected area diffraction (SAD) pattern from the region marked A.

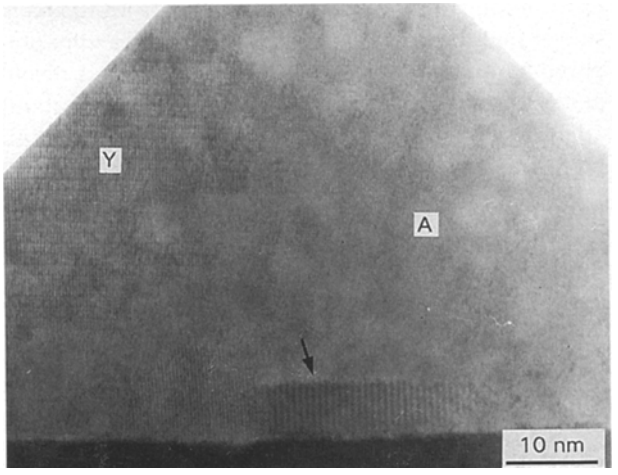

Figure 2 Cross-sectional high resolution TEM image of the as-deposited YBCO film.

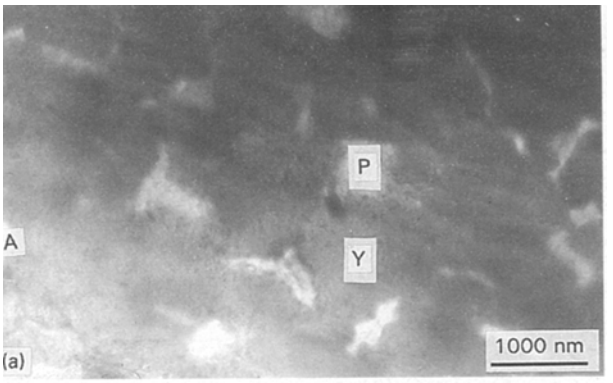

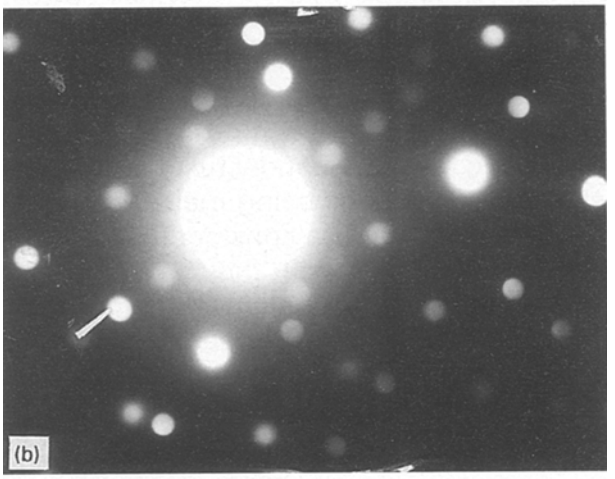

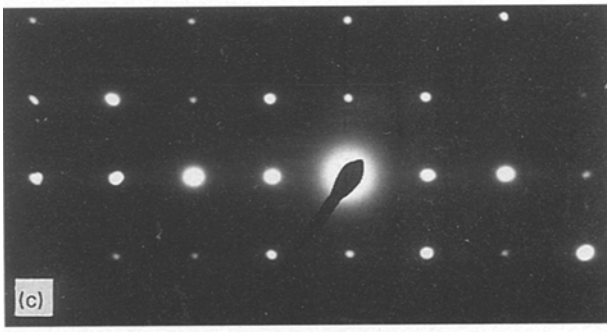

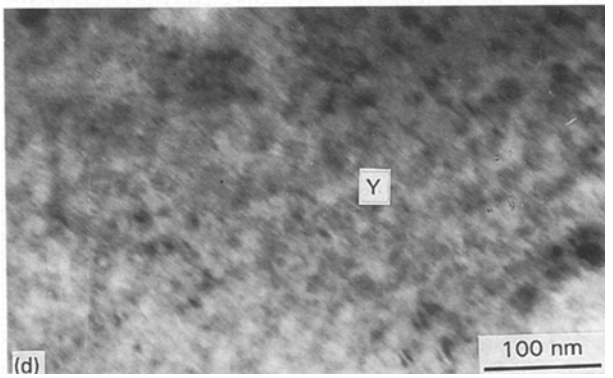

Figure 3 A group of plan view TEM micrographs and corresponding SAD patterns of the as-implanted YBCO film: (a) lower magnitude TEM image, (b) SAD pattern from the region marked P on Fig. 3a, (c) SAD pattern from the 1 2 3 phase marked Y on Fig. 3a, (d) and (e) a higher magnitude TEM image and corresponding SAD pattern from a second region of the 1 2 3 phase in the irradiated film.

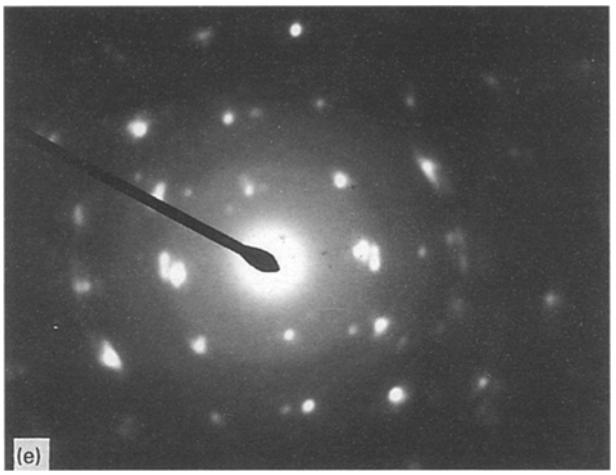

Figure 3 Continued

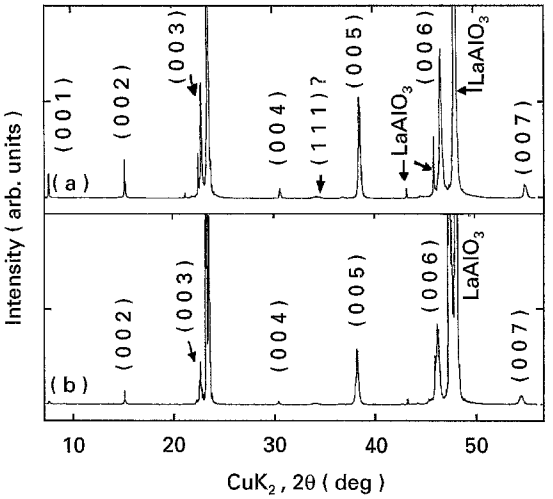

Figure 4 X-ray diffraction patterns from the as-deposited YBCO film (a) and the as-implanted film (b).

amorphous islands (marked P in Fig. 3a) can be seen in this TEM image. A selected area diffraction pattern of the polycrystalline area is shown in Fig. 3b. Most of the irradiated film is either still *c*-axis orientated single crystal or textured, i.e. diffraction spots becoming wider, due to defects and strain, as indicated by two typical selected area diffraction patterns from the film (see Fig. 3c, e). Fig. 3d shows a higher magnification image. It should be noted that in order to obtain this optimum contrast for the damage characteristic, the sample has been slightly tilted during this TEM observation. Some defects and associated strain contrasts (such as the mottled appearance) can be observed on Fig. 3d, probably this is a consequence of oxygen disordering due to the irradiation. This implantation also makes the film textured, as shown by Fig. 3e. The superconductivity of the film was completely destroyed by this implantation. X-ray diffraction (XRD) patterns show peak shift of the 1 2 3 phase and a decrease of the normalized intensities of the peaks of the 1 2 3 phase as shown in Fig. 4. The calculation shows that the *c*-axis lattice length of the film, as determined from room temperature XRD data, increased following this implantation from 1.168 to 1.179 nm, which corresponds to the oxygen content of $YBa_2Cu_3O_{7-\delta}$ decreasing from about 6.9 to 6.2 [6]. This change implies that about 4×10^{21} atoms cm^{-3} of oxygen were removed from the 1 2 3 phase during implantation. The loss of the superconductivity could also be due to damaging of the oxygen sublattice, i.e. oxygen disordering. A secondary ion mass spectroscopy (SIMS) ^2H depth profile from a similar sample [7] shows that $\sim$200 nm YBCO film will contain about 5% of the trapped ^2H after implantation. The simulated displacement per atom (d.p.a.) calculated by the transport of ion in matter (TRIM) code gives values which vary from 0.015 to 0.08 [8].

Fig. 5 shows a cross-section image of a sample after implantation and RTA at 870 °C for 20 s. Most of the film is still *c*-axis orientated. Some bright islands can be found in the film (indicated by an arrow). The diffraction pattern from these regions (shown in an insert) still shows a mainly polycrystalline structure. The T_c of this sample recovered to 82 K after annealing and XRD shows partial recovery of the *c*-axis

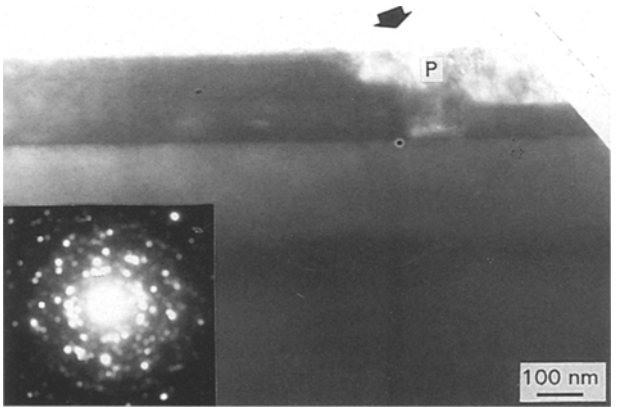

Figure 5 Cross-sectional TEM image of the YBCO film after implantation plus rapid thermal annealing (RTA) at 870 °C for 20 s and corresponding SAD pattern (insert) from region marked P on Fig. 3a.

length. This implies that the T_c change is not due to the structural change of the islands, but mainly due to the structural change of oxygen sublattice, i.e. oxygen reordering during RTA. It is very likely that during this high temperature RTA treatment the film absorbed oxygen from the O_2 ambient. Further results for optimizing RTA conditions will be reported elsewhere.

4. Conclusions

There is a considerable number of amorphous islands in the sputtered *c*-axis orientated YBCO films, These islands are Y rich and Cu poor compared with the 1 2 3 phase. After high dose H implantation, the amorphous islands crystallized. This implantation destroyed the superconductivity in the film, as characterized by T_c and made the film more granular, with the mainly epitaxial crystalline structure being maintained. After annealing, the implanted sample at 870 °C for 20 s, the islands are still polycrystalline and T_c has recovered to 82 K. This suggests that the change in T_c is not due to the structural change of

the islands, but mainly due to structural change of the oxygen sublattice.

Acknowledgement

This work has been supported by UK Engineering and Physical Science Research Council.

References

1. F. M. SABA, J. A. KILNER, T. J. TATE, M. J. LEE, J. W. RADCLIFFE, L. F. COHEN, P. G. QUINCEY, R. E. SOMEKH and P. PRZYSLUPSKI, *J. Alloys and Compounds* **195** (1993) 141.
2. J. W. RADCLIFFE, L. F. COHEN, G. K. PERKINS, A. D. CAPLIN, T. J. TATE, M. J. LEE, F. M. SABA, P. G. QUINCEY, R. E. SOMEKH and P. PRZYSLUPSKI, *ibid.* **195** (1993) 467.
3. X. X. XI, G. LINKER, O. MEYER, E. NOLD, B. OBST, F. RATZEL, R. SMITHEY, B. STREHLAU, F. WESCHENFELDER and J. GEERK, *Z. Phys.* **B74** (1989) 13.
4. Y. H. LI, C. LEACH and P. G. QUINCEY, *J. Mater. Sci. Lett.* **14** (1995) 670.
5. A. CATANA, R. F. BROOM, J. G. BEDNORZ, J. MANNHART and D. G. SCHLOM, *Appl. Phys. Lett.* **60** (1992) 1016.
6. A. KULPA, A. C. D. CHAKLADER, G. ROEMER and P. L. WILLIAMS, *Supercond. Sci. Technol.* **3** (1990) 483.
7. YUPU LI, J. A. KILNER, T. J. TATE, M. J. LEE, F. M. SABA, L. F. COHEN, A. D. CAPLIN and P. G. QUINCEY, *J. Appl. Phys.* **75** (1994) 4081.
8. J. F. ZIEGLER, J. P. BIERSACK and U. LITTMARK, "The stopping and ranges of ions in solids" (Pergamon, New York, 1985) p. 1.

Received 25 April
and accepted 24 May 1995